Conference Proceedings

Solar World Congress 2015
Daegu, Korea, 08 – 12 November 2015

Comparison-based Study on A Novel Point and Line Coupling-focus Solar Tower System Employing Linear Fresnel Heliostats

Yanjun Dai, Xian Li

Institute of Refrigeration and Cryogenic Engineering, Shanghai (China)

Abstract

The design and analysis of a beam-down solar tower system represents an extremely complex problem due to its performance dependent on various interrelated factors. A novel heliostat with linear Fresnel reflecting technology is employed in the beam-down solar tower and investigated theoretically in this paper, being its superior wind-resistance performance compared with convectional heliostat. In order to investigate the concentrating principle of linear Fresnel heliostat, a comparison-based study of these parameters and efficiencies is implemented herein. The effects of the hyperboloid eccentricity on both the sun-shape and the geometry of the heliostat are analyzed. The effect of the aberration in optics for the linear Fresnel heliostat on the image at the focal plane has been investigated.

Keywords: *Point and line coupling-focus solar tower, beam-down, linear Fresnel heliostat, optical analysis*

1. Introduction

It is well known that the energy and environmental crisis has been promoting the development of solar thermal technologies, where concentrating solar tower technology has been proven to be a fairly efficient way of converting solar energy into thermal energy or electricity (Kalogirou, 2004). As for the traditional concentrating solar tower, solar energy from a large array of heliostats is focused onto a tower that captures the heat by a receiver, and then converts that heat to electricity using a steam generator and a steam turbine. However, it can be pretty expensive in terms of building a low heat-loss tower and pumping heat transfer fluid (HTF) such as molten salt up to the tower top which usually mounted at hundred meters high to the ground. In order to overcome these shortcomings, beam-down solar tower (BST) has been proposed and developed, where a second set of beam-down concentrator (BC) directs the solar radiation back down to a central receiver (CR) placed on the ground, instead of having the heat-capturing system up at a high tower. On account of aforementioned merits BST technology is considered as one of the promising ways to harvest solar energy and is worth continuing research.

A variety of studies on optical performance of various BST systems are in the literature. The concept of BST was proposed for the first time by Rabl (1976) and then developed at the Weizmann Institute in Israel (Segal and Epstein, 1997). Segal and Epstein (1999, 2000, 2003) described the optics of the BST system, where two types of secondary reflectors, hyperboloid and elliptical were investigated for a comparative study. However, a single solar ray per heliostat was considered, and shading and blocking effects have been neglected. Detailed optical analysis of BST systems with the hyperboloid concentrators and the compound parabolic concentrator (CPC) have been performed (Leonardi, 2012; Wei et al., 2013), but solar flux distribution on the absorber surface of the CR have not been involved.

In this paper, a BST system employing strong wind-resistance linear Fresnel concentrating technology which is named as point-line-coupling-focus (PLCF) system, is introduced and investigated theoretically. Based on the MCRT, the optical analysis model of PLCF system is developed considering the incident angle, solar position, optical errors, and sun-tracking angles. Comparison-based study on the optical performance between PLCF and convectional systems is implemented.

doi:10.18086/swc.2015.04.05 Available at http://proceedings.ises.org

2. PLCF system description

A schematic of concentrating concept of BST including a linear Fresnel heliostat and a beam-down concentrator (BC) is shown in Fig. 1. A hyperboloid reflector is used as the BC. The incident rays hit on the surfaces of Linear Fresnel heliostat facets. The heliostat tracks sun and reflects incident rays to the BC, and then these rays are concentrated downwards to the final focal point at the focal plane. The concentrating process of this BST is mainly composed of focusing effects of heliostat and BC. The detailed parameters of linear Fresnel heliostat has been introduced by Li et al. (2015). As shown in Fig. 1, l_m and H_h are the length and the height of the linear Fresnel heliostat, respectively. D is the distance between the heliostat and the cavity receiver. H and H_{max} are the height of point A and the maximum height of the hyperboloid reflector, respectively. F_1 and F_2 are the upper focus (target point) and lower focus (focal point), respectively. r_{max} is the maximum radius of the hyperboloid reflector.

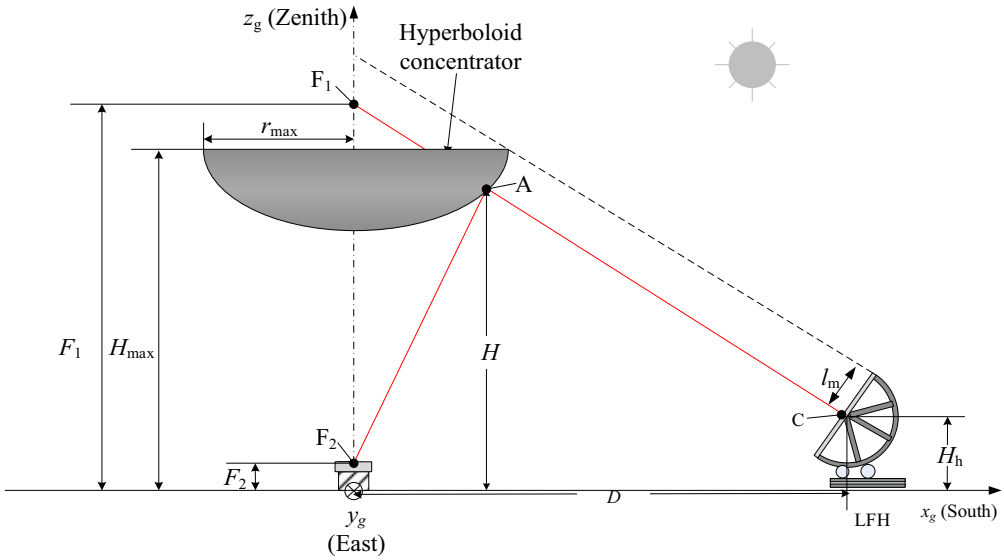

Fig. 1: Schematic diagram of geometric parameters of the PLCF system with the hyperboloid concentrator

3. Optical analysis models

3.1. Sunshape

Because sun rays are not strictly parallel, the sun rays hitting on the surface of the sub-mirror are modelled as a conic bundle where the rays of the bundle are weighted with a non-uniform energy distribution. Based on the concept of sun-shape profile, the intensity distribution I of solar disk proposed by Johnston (1998) can be calculated as

$$I = I_o \frac{1+\beta\sqrt{1-\frac{\vartheta}{\vartheta_s}}}{\pi\vartheta_s^2\left(1+\frac{2\beta}{3}\right)} \qquad \text{(eq. 1)}$$

where ϑ denotes the angle of a surface element on the solar sphere, I_o is the intensity in the center of the solar disk, β is the limb darkening parameter.

3.2. Normal vector of optical surface

The normal vector ($\mathbf{N_F}$) of the optical surface where rays currently hit is expressed by a unified differential formula (Cui et al., 2012) derived from surface equations f of the investigated geometric surface:

$$\mathbf{N_F} = \begin{bmatrix} f_x \\ f_y \\ f_z \end{bmatrix} = \begin{bmatrix} \dfrac{\partial f(x_g, y_g, z_g)}{\partial x_g} \\ \dfrac{\partial f(x_g, y_g, z_g)}{\partial y_g} \\ \dfrac{\partial f(x_g, y_g, z_g)}{\partial z_g} \end{bmatrix} \quad \text{(eq. 2)}$$

3.3. Optical surface errors

It is generally assumed that all surface errors follow a Gaussian distribution (Rabl, 1985) characterized by the standard deviation. The variances of each individual error distribution can be summed to one total equivalent variance, σerr, which describes the composite effect of all errors, namely the specularity error, the slope error, the shape error, the alignment error, and the tracking error. The simple Rayleigh method of surface error (Cooper and Steinfeld, 2011) for generating surface error is given as

$$\theta_{err} = \sigma_{err}\sqrt{-2\ln U} \quad \text{(eq. 3)}$$

$$\phi_{err} = 2\pi U \quad \text{(eq. 4)}$$

$$\mathbf{M}' = \cos\theta_{err}\mathbf{M} + \sin\theta_{err}\left(\sin\phi_{err}\mathbf{u}_x + \cos\phi_{err}\mathbf{u}_y\right) \quad \text{(eq. 5)}$$

where ζ_{err} and ϕ_{err} are defined as the azimuthal angular and circumferential components of the surface error, respectively. U is the random number with uniform distribution in the interval of 0 and 1. M′ is deviant reflected vector with surface error. $\mathbf{u_x}$ and $\mathbf{u_y}$ are unit vectors in the Cartesian x-component and y-component directions, respectively.

3.4. Concentration ratio

The concentration ratio is defined as

$$C = \frac{A_h}{A_{sp}} \quad \text{(eq. 6)}$$

where A_h and A_{sp} represent the total aperture area of heliostat field and the spot area at the lower focal plane.

3.5. Optical efficiency

Optical performance index Optical efficiency of the BCST system is related to significant factors involving cosine efficiency ε_{cos}, shading and blocking efficiency ε_{sb}, interception efficiency ε_{it}, and the atmospheric attenuation efficiency ε_{aa}. Instantaneous optical efficiency with respect to above efficiencies, proposed by Schmitz et al. (2006), is expressed as

$$\eta_o = \eta_{cos}\eta_{sb}\eta_{it}\eta_{aa}\rho_h\rho_{BC} \quad \text{(eq. 7)}$$

where ρ_h and ρ_{BC} indicate the reflectance of LHF and BC, respectively.

4. Results and discussion

4.1. The effect of the structure of hyperboloid reflector

As shown in Fig. 2, the optical surface of hyperboloid reflector is mainly affected by the eccentricity e and the upper and lower focuses. Considering F_1 = 75m and F_2 = 5m, the effect of e on the hyperboloid structure is analyzed. Fig. 2(a) shows the relationship between e and the maximum radius r_{max}. As shown in Fig. 2(a), the r_{max} increases with the increase of the eccentricity e which shows an increasing trend. When e > 50, the increase of r_{max} is limited and trends to be stable. In addition, the distance D increases with the increase of r_{max}. Fig. 2(b) reveals the effect of e on the hyperboloid surface. As can be seen, under the identical conditions, the size of the hyperboloid surface increases with the increasing e. When e trends to infinity, hyperbolic mirror transfers to be the plane mirror.

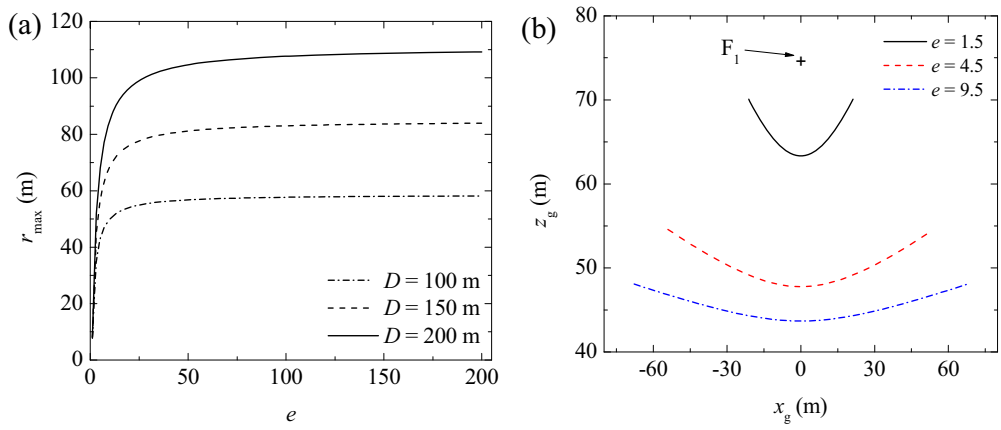

Fig. 2: The effects of D and e of geometric parameters on the shape of the hyperboloid reflector: (a) the maximum radiu r_{max} as a function of e; (b) the effect of parameter e

In this case, the magnification M is the ratio of the image size of the upper focal plane to the image size of lower focal plane. Based on the optical analysis of MCRT method, considering sun angle effects, the single ray reflected from point C is used to reveal characteristics of the spot on the lower focal plane. Fig. 3 shows the effects of D and e on the spot characteristics of a single ray reflected from the geometric center of heliostat. Fig. 3(a) shows the effect of the parameters of e and D on the spot sizes of the upper and lower focal planes. With the increase of e, the spot size of lower focal plane decreases. When e trends to infinity, the spot size of the focal plane trends to be the same. Fig. 3(b) is the relationship between e and M which increases sharply with the increase of e from 1 to 4.5, and the amplification factor decreases sharply. Therefore, the increase of D in a certain extent can weaken the negative effect caused by the magnification of the hyperboloid mirror, and can improve the concentration ratio. The comparison-based results show that the MCRT optical analysis model developed in this paper has the reasonable accuracy.

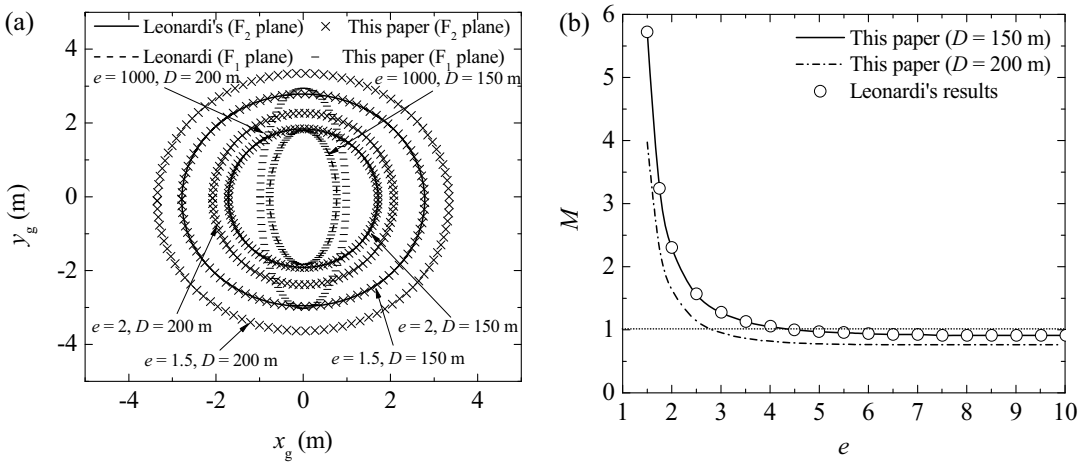

Fig. 3: The effects of *D* and e on the spot characteristics of a single ray reflected from the geometric center of heliostat: (a) the effect on the spot size; (b) the effect on the magnification *M*

4.2. The effect of structure parameters of linear Fresnel heliostat

The effect of heliostat structure parameters on optical properties is analyzed under the conditions of H_h=5m, F_1 = 75 m, F_2 = 5 m, r_{max} = 44.1 m, γ = 0°, α = 90°, D = 150 m, e = 3. With the diameter of 10 m of the circular heliostat (as shown in Fig. 4), the linear Fresnel heliostat is divided into five mirrors.

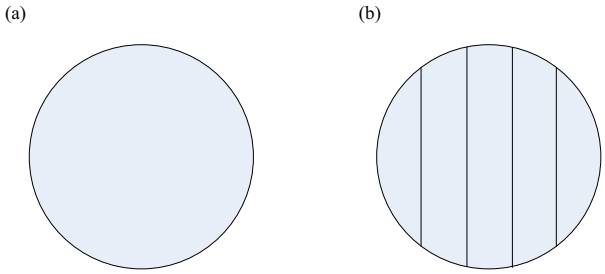

Fig. 4: Schematic diagram of heliostats: (a) convectional circle-plate heliostat (CH); (b) circle linear Fresnel heliostat (diameter of 10m)

Fig. 5 shows comparison results of the spot sizes of LFH and CH at the upper and lower focal planes. As shown in Fig. 5, the LFH has the smaller spot sizes compared to CH.

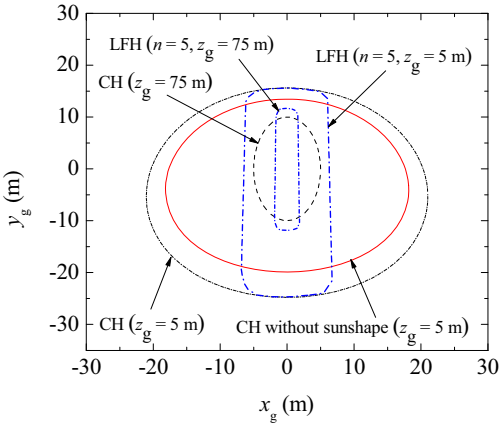

Fig. 5: Comparison results of the spot sizes of LFH and CH at the upper and lower focal planes

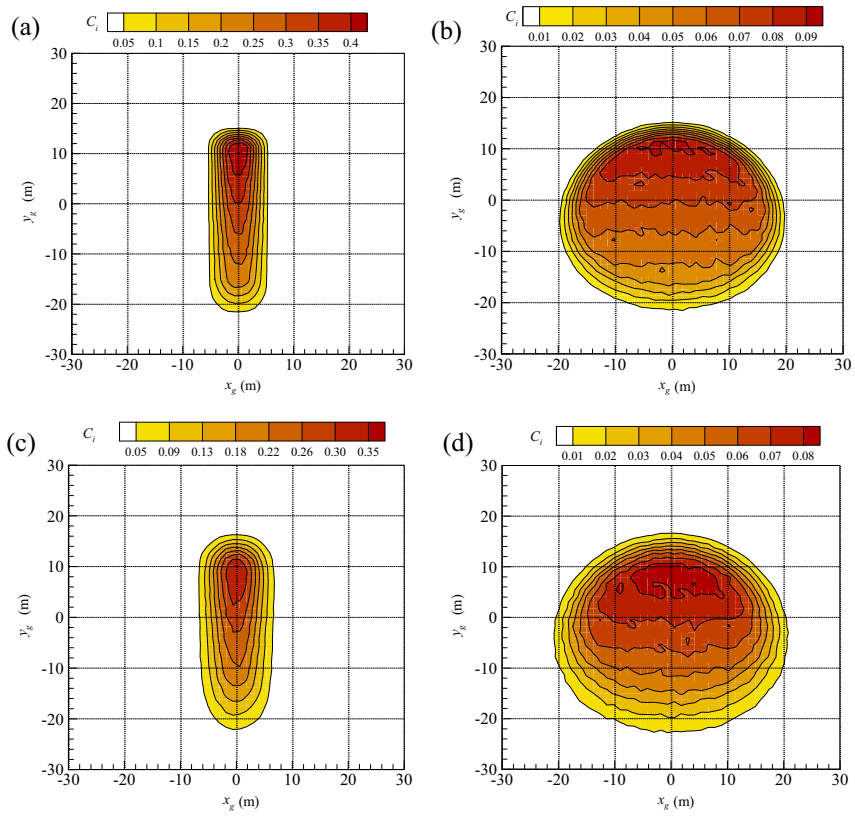

Fig. 6: Comparison results of the local concentration ratio of the spot for LFH and CH: (a) LFH without optical error; (b) CH without optical error; (c) LFH with optical error; (d) CH with optical error (σ_{err} = 3.5 mrad)

Concentrating ratio C is an important index to evaluate the solar concentrating characteristics. Fig. 6 shows comparison results of the local concentration ratio of the spot for LFH and CH. The effect of optical errors has been considered herein. Analysis shows that the linear Fresnel heliostat has obvious advantages in concentrating ratio. Comparative analysis of optical error of focal spot local concentration ratio can be found and certain extent increase of the focal spot size causes the decrease in concentrating ratio. However, the differences in local concentration ratio distribution between two heliostats are extremely limited.

4.3. The effect of structure parameters of heliostat mirror

The shape of the heliostat mirror has an important effect on the focusing performance. Here, the spot sizes of various length-width ratios are investigated with D = 150 m and e = 3. Fig. 7 reveals the effect of length-width ratio on the characteristic of the spot at the lower focal plane. The diameter of CPC is 20 m. Fig. 7(a), 7(b), and 7(c) represent the length-width ratios of 1:1, 5:1, and 2:1, respectively. As can be seen, when the length-width ratio is 1:1, the LFH has the highest optical efficiency of 73.1%.

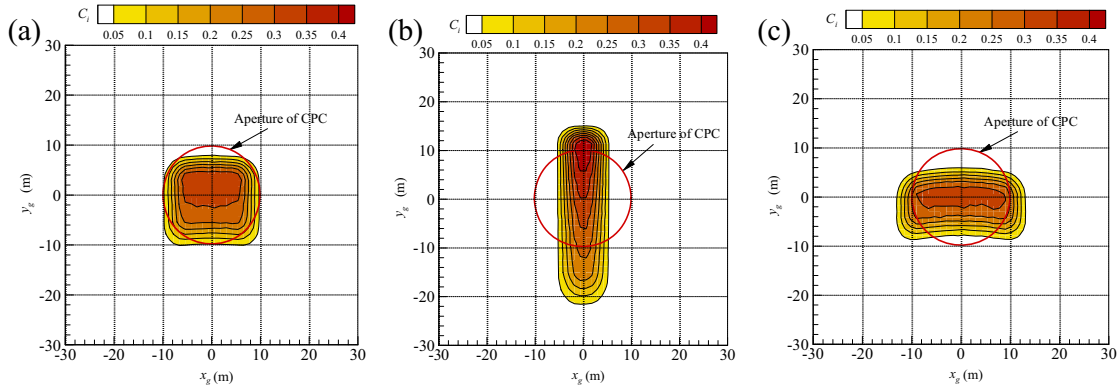

Fig. 7: The effect of length-width ratio on the characteristic of the spot at the lower focal plane: (a) length-width ratio of 1:1 with spillage loss of 26.9%; (b) length-width ratio of 5:1 with spillage loss of 41%; (c) length-width ratio of 2:1 with spillage loss of 31.2%

4.4. Comparison-based analysis of optical efficiency

The comparison-based analysis of optical efficiency is implemented considering the shape of heliostat shown in Fig. 8. Fig. 9 shows the effect of the solar position and design parameters on the cosine efficiency as well as the shading and blocking efficiency. The aperture area of heliostat is 100 m^2 facing south with the coordinates (-150, 0, 5). The parameters of hyperboloid reflector is e = 3, F_2 = 5 m. The aperture radius of CPC is 11 m.

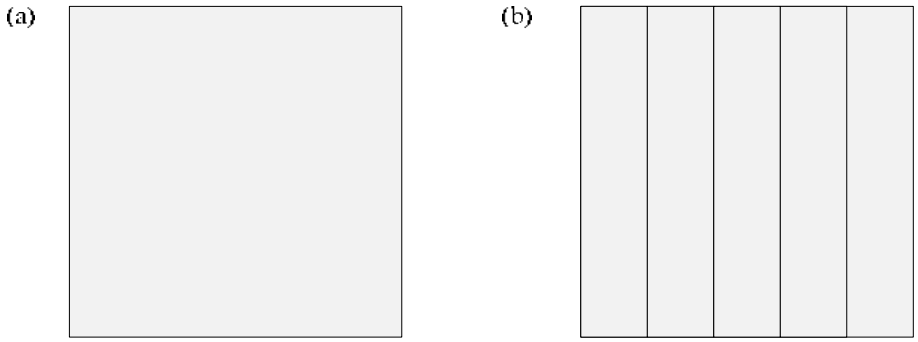

Fig. 8: Schematic diagram of heliostats: (a) convectional rectangle-plate heliostat; (b) rectangle linear Fresnel heliostat

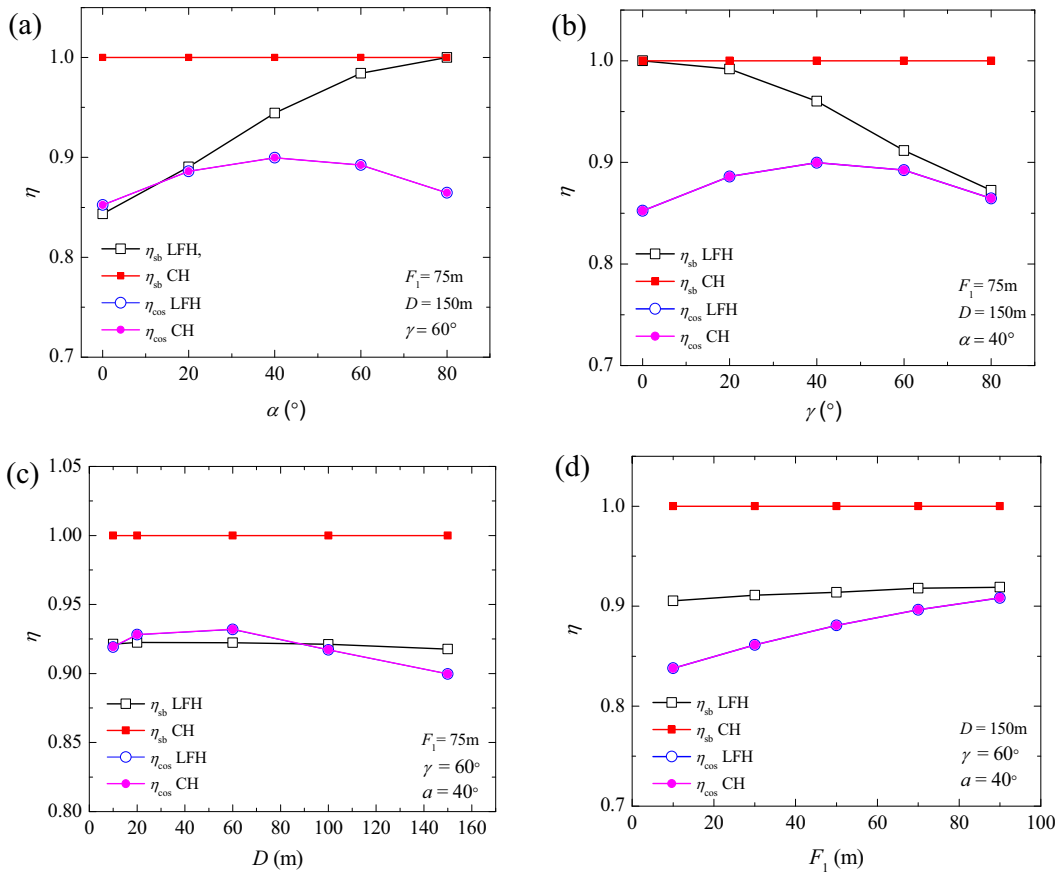

Fig. 9: The effect of the solar position and design parameters on the cosine efficiency as well as the shading and blocking efficiency: (a) the effect of solar altitude; (b) the effect of solar azumith; (c) the effect of the distance D; (d) the effect of the upper focus F1

As shown in Fig. 9, LFH and CH have the identical cosine efficiency which is not affected by the parameters of solar position and D. In addition, the LFH has a greater impact than CH with respect to the effects of solar position (solar angles) on shading and blocking efficiency. As shown in Fig. 9(c) and 9(d), the parameters of D and F_1 have limited impact on the shading and blocking efficiency. The effect of the shape of mirror (shown in Fig. 10) on the optical efficiency is studied herein.

Fig. 10: The structures of LFH and CH with the identical area

Under the conditions of the aperture radius of 4.9 m, the solar altitude of 82°, the aperture area of the heliostat of 100 m^2 facing south, the coordinates (-150, 0, 5). The parameters of hyperboloid reflector (e = 3, F_1 = 75 m, F_2 = 5 m), the detailed comparison results are listed in Table 1. As can be seen, the shading and blocking efficiency of LFH is slightly lower than that of CH, however, the interception efficiency of LFH is obviously superior than that of CH. Thus, the optical efficiency of LFH is approximately 3.4 times the optical efficiency of a CH. In addition, the length-width ratio of 1:1 has the optimal optical efficiency.

Tab. 1: Comparison results of the optical efficiency of LFH and CH solar thermal system under various solar azimuth

Solar azimuth	LFH				Rectangular mirror				Square mirror			
	η_{cos}	η_{sb}	η_{it}	η_{o}	η_{cos}	η_{sb}	η_{it}	η_{o}	η_{cos}	η_{sb}	η_{it}	η_{o}
0°	0.879	1	0.968	0.620	0.879	1	0.202	0.130	0.879	1	0.281	0.180
20°	0.877	1	0.970	0.620	0.877	1	0.210	0.130	0.877	1	0.290	0.185
40°	0.870	1	0.972	0.616	0.871	1	0.217	0.133	0.871	1	0.295	0.187
60°	0.861	1	0.973	0.611	0.861	1	0.221	0.139	0.861	1	0.31	0.195
80°	0.849	0.998	0.973	0.601	0.849	1	0.230	0.142	0.849	1	0.32	0.198

5. Conclusions

A novel heliostat with linear Fresnel reflecting technology is employed in the beam-down solar tower and investigated theoretically in this paper, being its superior wind-resistance performance compared with convectional heliostat. The comparison-based study on the convectional heliostat and linear Fresnel heliostat is implemented. Following conclusions can be drawn:

(1) Analysis results shows that the linear Fresnel heliostat has obvious advantages in concentrating ratio and spot size.

(2) The shape of the heliostat mirror has an important effect on the focusing performance. The optimal length-width ratio is 1:1 in order to achieve the highest optical efficiency.

(3) Under the same conditions, the optical efficiency of LFH is approximately 3.4 times the optical efficiency of a CH.

6. Acknowledgements

This work was supported by National Natural Science Foundation Project of China under the Contract No. 51276112.

7. References

Cooper, T., Steinfeld, A., 2011. Derivation of the angular dispersion error distribution of mirror surfaces for Monte Carlo ray-tracing applications. Journal of Solar Energy Engineering, 133(4), 044501–044504.

Cui, F.Q., He, Y.L., Cheng, Z.D., Li, D., Tao, Y.B., 2012. Numerical simulations of the solar transmission process for a pressurized volumetric receiver. Energy 46(1), 618–628.

Johnston, G., 1998. Focal region measurements of the 20 m2 tiled dish at the Australian national university. Sol. Energy 63(2), 117–124.

Leonardi, E., 2012. Detailed analysis of the solar power collected in a beam-down central receiver system. Sol. Energy 86, 734–745.

Li, X., Dai, Y.J., Wang, R.Z., 2015. Performance investigation on solar thermal conversion of a conical cavity receiver employing a beam-down solar tower concentrator. Sol. Energy 114, 134 – 151.

Rabl, A., 1976. Tower reflector for solar power plants. Sol. Energy 18, 269–271.

Rabl, A., 1985. Active solar collectors and their applications. New York: Oxford University Press.

Segal, A., Epstein, M., 1997. Modelling of solar receiver for cracking of liquid petroleum gas. J. Sol. Energy Eng. 119, 48–51.

Segal, A., Epstein, M., 1999. Comparative performances of ‘tower-top’ and ‘tower reflector’ central solar receivers. Sol. Energy 65, 207–226.

Segal, A., Epstein, M., 2000. The optics of the solar tower reflector. Sol. Energy 69, 229–241.

Segal, A., Epstein, M., 2003. Optimized working temperatures of a solar central receiver. Sol. Energy 75, 503–510.

Schmitz, M., Schwarzbozl, P., Buck, R., Pitz-Paal, R., 2006. Assessment of the potential improvement due to multiple apertures in central receiver systems with secondary concentrators. Sol. Energy 80(1), 111–20.

Wei, X.D., Lu, Z.W., Yu, W.X., Xu, W.B., 2013. Ray tracing and simulation for the beam-down solar concentrator. Renewable Energy 50, 161–167.